

# Wind pressure on elementary building forms evaluated by model tests

Among the least understood of the forces dealt with by the structural engineer is wind pressure. Evidence of this fact is the common design practice of using an arbitrarily chosen uniform pressure intensity over the projected area of a structure or member. Students of fluid motion are well aware of the great variation in pressure that results from the flow of air around any object, and they realize that knowledge of the actual pressure distribution around buildings would permit more economical—yet safer—designs. Although tests have been conducted by many investigators in the past fifty years, the technical literature contains no comprehensive experimental data that would permit interpolation for wind loads at particular points on buildings of any desired form. This situation is partially due to the great divergence in building forms, but in large measure it has resulted from the failure of structural engineers as a whole to appreciate the need for such information.

In 1946 a systematic series of tests on three-dimensional building models was begun at the University of Iowa for a graduate thesis in the Department of Mechanics and Hydraulics. The scope of these tests was later broadened as a project of the Iowa Institute of Hydraulic Research, sponsored by the Office of Naval Research.

## Theoretical Considerations

The variation in pressure around a building depends on the local variations in velocity in accordance with the fundamental energy relationship,

$$p - p_o = \frac{\rho v_o^2}{2} - \frac{\rho v^2}{2}$$

in which  $p$  and  $v$  are the pressure intensity and velocity at any point, and the subscript "o" indicates a point at some distance from the building in the undisturbed air stream. The density  $\rho$  varies from 0.0027 slugs per ft<sup>3</sup> at 0 deg F to 0.0022 slug per ft<sup>3</sup> at 100 deg F.

If the difference  $\Delta p$  between the pressure at any point and that in the undisturbed flow is divided by  $(\rho v_o^2)/2$ , the expression takes the form,

$$\frac{\Delta p}{(\rho v_o^2)/2} = 1 - \left(\frac{v}{v_o}\right)^2$$

from which the effect of a local change in the velocity is at once apparent. The pressure parameter has its maximum positive value of unity at a point of stagnation, whereas its negative value has no definite limit. The parameter

$$\frac{\Delta p}{(\rho v_o^2)/2}$$

is essentially a pressure coefficient and will hereafter be referred to as  $C_p$ .

The velocity variation is uniquely determined by the flow pattern around the building. This pattern depends on the geometrical configuration of the building, the velocity distribution of the wind, and the viscosity of the air. Although each of these factors must generally be considered, it can be demonstrated that the geometry is nearly always the dominant one. Reduction of wind velocity near the ground has the primary effect of causing smaller pressure variations than would otherwise occur. Consequently, tests

made in an air stream of constant velocity will indicate the maximum pressure variation to be expected. Viscosity likewise influences the flow pattern in some cases, but the artificial roughening of curved models or the sharp discontinuities that usually exist serve to produce a constant flow pattern which is practically independent of viscous effects.

Therefore it may be assumed that the values of  $C_p$  obtained on models tested in the wind tunnel and displaying flow patterns of constant form, with fixed points of separation, may be used to predict actual pressures on prototype structures.

## Low-Velocity Wind Tunnel Tests

The tests were performed in a low-velocity wind tunnel having a test section 6 ft wide and 4 ft high. Models were mounted on a thin platform 6 in. above the floor in a region of constant velocity. The models were made of 1/8-in. plastic plate and were formed into the series of unit combinations shown in Fig. 1. Piezometer openings 1/16 in. in diameter were closely spaced in regions where high velocity gradients were expected and were provided with nipples for tubing connections. The basic forms tested were the hangar or semi-cylinder, the rectangular vertical wall, and the block-type gabled building. The rectangular block-type buildings consisted of 4 X 4 X 2-in. blocks in combination with others of that size or of 4 X 8 X 2-in. size to form buildings with length-width ratios of 1, 2, and 4 in combination with height-width ratios of 1/2, 1, and 3/2. In addition, each of these combinations had gable roofs whose inclinations to the horizontal ranged from 15 to 45 deg.

tudes at any point. They do not, however, provide a ready means of comparing the effects of varying geometrical configuration. For this purpose, pressure profiles at significant sections were plotted for windward and leeward wall and roof surfaces.

A typical summary of pressure variation on a hangar roof is shown in Fig. 3. It is apparent that negative pressures over the central section of the hangar roof are significantly increased as the length of the building becomes greater. See curve (b). Because of the lightness of hangar-type structures, lift and drag coefficients were also determined for use in the formulas,

$$F_L = C_L LD \frac{\rho v_0^2}{2}$$

$$F_N = C_N LD \frac{\rho v_0^2}{2}$$

$$F_A = C_A \pi D^2 \frac{\rho v_0^2}{16}$$

Each of the three basic forms was tested at several orientations with the wind, the angle  $\alpha$  being measured between the end wall and the wind vector, as indicated in Fig. 1. There were 16 tests on hangar forms, 21 on rectangular walls, and 108 on block forms. In addition, exploratory tests were made to determine the effect of spacing on the pressures over the facing walls of identical flat-roofed buildings with parallel orientation.

Pressures were measured with a delicate Wahlen differential gage which was sensitive to 0.00003 psi. The reference value  $(\rho v_0^2)/2$  was measured by means of a stagnation tube and a floor piezometer near the model platform. Pressures on the models were read relative to the same floor piezometer. The ratio of these readings gave the value of  $C_p$ . The probable error in the pressure determinations was less than 2 percent.

Test results were plotted on the developed surfaces of the models and lines drawn through points having equal values of  $C_p$  to yield patterns similar to those in Fig. 2. Integration of the pressure patterns yielded the total force acting on any surface. Values of the parameter  $C_p$  are directly useful, as previously indicated, to determine the actual pressure distribution on a similar structure at any desired wind velocity. Such diagrams for each of the 150-odd test conditions are presented in the complete report referred to at the end of this article.

Force Intensity Varies Widely

The pressure patterns indicate the wide variation of force intensity over the surface of a building and permit the evaluation of actual magni-

in which  $F_L$  is the lifting force;  $F_N$  and  $F_A$  the horizontal components of the drag in the normal and axial directions, respectively;  $C_L$ ,  $C_N$ , and  $C_A$  are lift and drag coefficients; and  $L$  and  $D$  are the length and diameter of the structures. The maximum  $C_L$  value of 0.55 occurs on the longer models at wind angles of 30 deg. The coefficient  $C_N$  rises to 0.84 at the same wind angle, whereas the coefficient  $C_A$  reaches 1.18 on the shortest model with the wind directed toward the end face. The greatest vectorial combination of the drag coefficients is 1.23.

Pressure patterns on the vertical wall forms disclose that the geometric shape has a pronounced effect on pressure intensity, as illustrated in Fig. 4. The pressure patterns were integrated to determine the total force acting on the windward

Models of buildings were made from 1/8-in. plastic sheet and equipped with 1/16-in. piezometers closely spaced at points where velocity gradients were high. The model shown was 4 x 4 in. in plan, with a 45-deg roof, the smallest size tested.

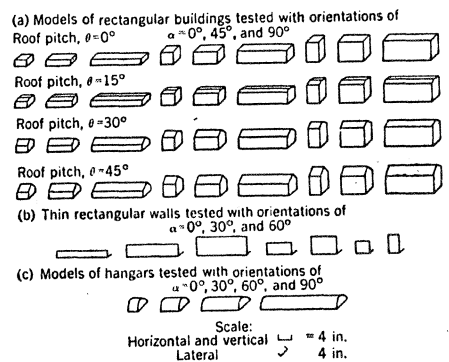


FIG. 1. Schedule of model arrangements shows shapes, proportions and wind directions at which models were tested. There were therefore 108 tests on block-type buildings, 21 tests on walls, and 16 tests on hangars.

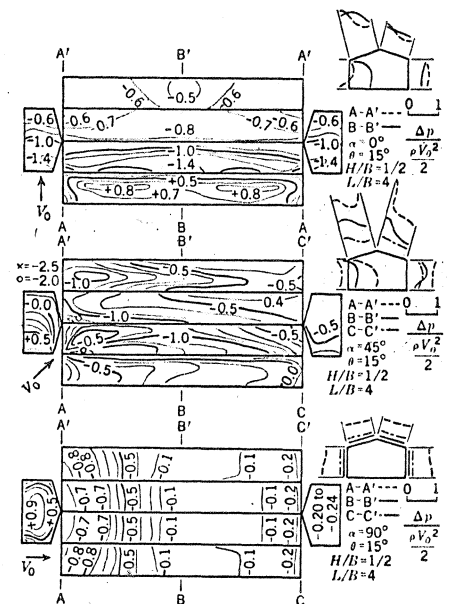
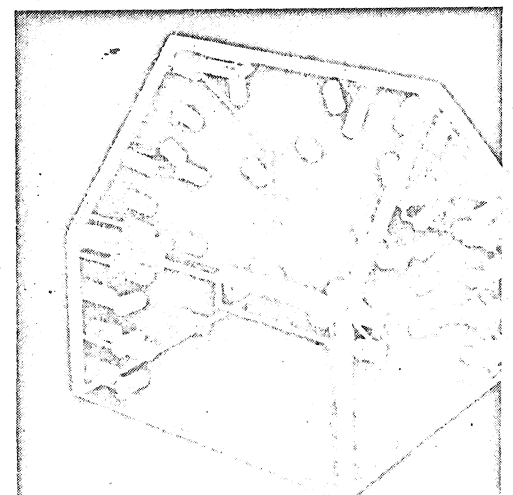


FIG. 2. Typical pressure patterns on block-type model are shown for three wind directions. Occurrence of negative pressure on all faces of building should be noted. Pressure profiles at right indicate variation at end and center sections.



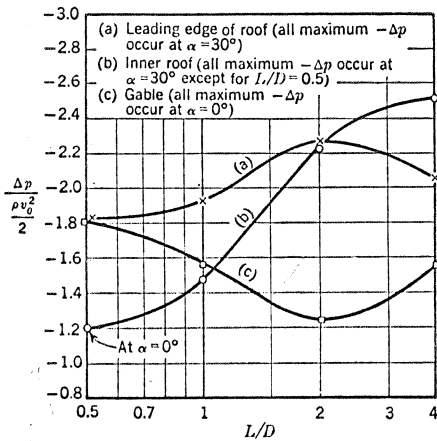
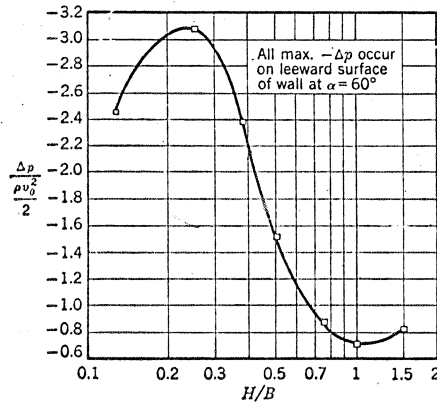


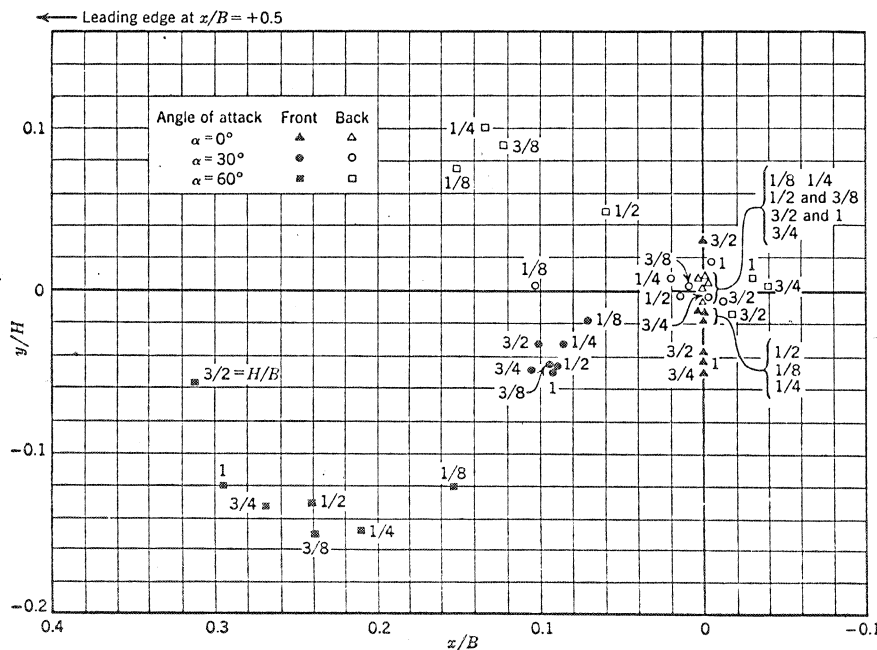
FIG. 3. Pressure intensities on a hangar vary with relative length of structure. Maximum pressure intensities are shown (a) at leading edge of roof when wind is at an angle, (b) at section where greatest vacuums occur, and (c) at end gable with a normal wind.



and leeward faces of the walls, and the position of the pressure centroid was located relative to the vertical and horizontal center lines of the wall, as shown in Fig. 5. Apparent from this figure is the considerable mismatching of the centers on opposite sides of the walls. This indicates the presence of a decided torque on the wall supports. The drag coefficients on the windward and leeward surfaces are of the same order of magnitude, typical values being 0.75 and -0.55. In combination, the total coefficient of drag ranged from 1.2 to 1.4.

The block-type structures had a greater variation in form than either the hangars or the walls and consequently were subject to greater pressure variations. The pressure profiles near the ends and at the centers of the buildings were compared with respect to both local pressure intensity and average pressure intensity over the section. Except for cases of symmetrical wind loads, each building face displayed a different pressure distribution. In general, the windward face was under positive pressure, approaching the stagnation value of  $(\rho v_0^2)/2$  near the center of the wall and decreasing to values below atmospheric pressure at the exposed edges. The

FIG. 4. Pressure intensity varies with proportions of wall. Largest vacuums occur on back side of wall with wind direction 60 deg from normal.



roof was generally subject to negative pressure on the windward slope if its inclination was small, and was invariably subject to negative pressure on the lee slope. The leeward and end walls, being in the eddy formed by separation at the leading edges of the building, were in a region of rather uniform negative pressure. As the wind direction varied, these general conditions were modified.

Variations in the geometry of the buildings do not cause large pressure variations in so far as building proportion is concerned (Fig. 6). Roof angle, however, is of considerable significance (Fig. 7). The variation of average positive pressure ranges from 0.75 to 0.95 of the stagnation value in all models, there being little relation to their proportions other than a slight tendency toward greater values at higher roof inclinations. Average negative pressures over sections near the corners showed even less effect of building proportions, but the rather large negative values on the windward face should be noted. Many engineers may find it hard to reconcile the presence of both positive and negative pressures on the windward face of a building, but the fact that both are present is well substantiated.

The angle of inclination has a major effect on pressure distribution over the roof (Figs. 7 and 8). The effect of roof inclination overshadows that of building proportion, although in general the long, high buildings were found to be subject to considerably higher negative pressures than the short, low forms.

The effect of roof inclination is even more pronounced if local pressure intensities are compared. The greatest negative pressure, regardless of wind direction, was plotted against the geometrical characteristics of the building (Fig. 9). The large suction that developed at roof angles of less than 30 deg, at the windward corner in a quartering wind, are truly surprising. Under these conditions, two vortices form over the roof and produce extremely low pressures. The peak value of -7.4, combined with stagnation conditions (+1.0) inside the building, would correspond to

FIG. 5. Centers of pressure on wall faces are not opposite except in normal wind. Hence, an appreciable twist is exerted on wall supports. Suction on back of wall is generally only 30 percent less than thrust on front side.

an uplift of 78 psf in a 60-mph wind, a value well in excess of usual design values.

The lee roof, lee wall, and end walls are subject to rather uniform underpressures averaging about  $0.6 (\rho v_0^2)/2$ . Although space does not permit the inclusion of summary curves, they are available in the original report.

#### Effect of Building Proximity

The last phase of the investigation dealt with the effect of building proximity. Since the number of tests required to establish the relations previously described was considerable, it was not feasible to investigate the effect of all the variables involved in a complete study of proximity effects. Only an exploratory series of tests was made to determine whether the presence of an adjacent building could increase the negative pressures measured on an isolated structure. Two identical flat-roofed buildings of equal width and height were placed side by side with their long sides parallel. Four lengths of buildings were tested at several different spacings and wind directions. For these particular buildings it was found that the greatest negative pressure intensities developed at the front edge of the passage between buildings and were approximately twice as large as the pressure at the same point on an isolated building when the spacing was about one-tenth that of the building width or height. Furthermore, the average suction on the facing walls was as much as three times that on a single building side wall. Because of the restriction of variables, the only conclusion reached was that the presence of an adjacent building may cause greater negative pressures on some areas of walls than would occur on the same walls were the building isolated. Particular arrangements should be studied in a wind tunnel to determine actual pressure distributions.

#### Example Shows Application

To indicate the use of the test results the following example is presented. Determine the wind loadings on a rectangular building  $20 \times 80$  ft in plan and 10 ft high with a roof slope of 1:4 and bents on 20-ft centers. (See Fig. 10.) The roof slope of 1:4 is 14 deg, near enough to 15 deg to permit direct use of tests in a model having  $\theta = 15$  deg,  $L/B = 4$ , and  $H/B = 1/2$ , the pressure contours of which are shown

FIG. 6. Average pressure on front wall of rectangular building is positive near center of structure but negative at corners. Building proportions do not greatly affect front-wall pressures.

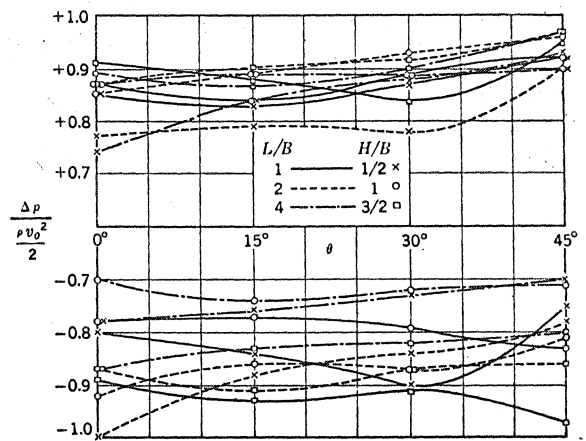


FIG. 7. Average negative pressures at worst sections of windward roof show decided effect of roof pitch. Greatest uplift occurs at leading edge of flat-roofed buildings or at ridge of steep roofs.

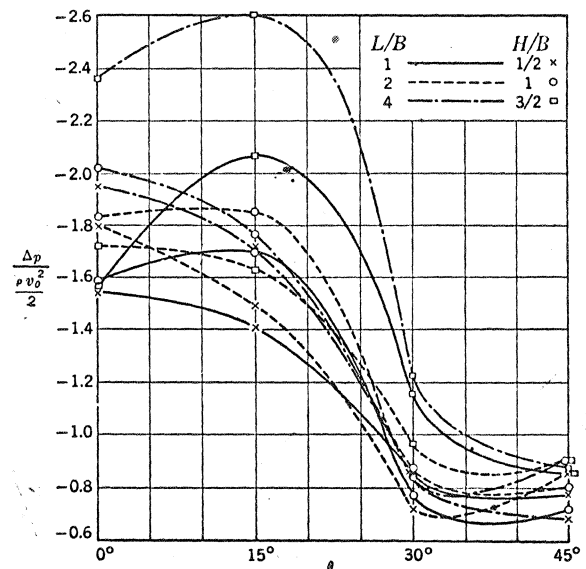
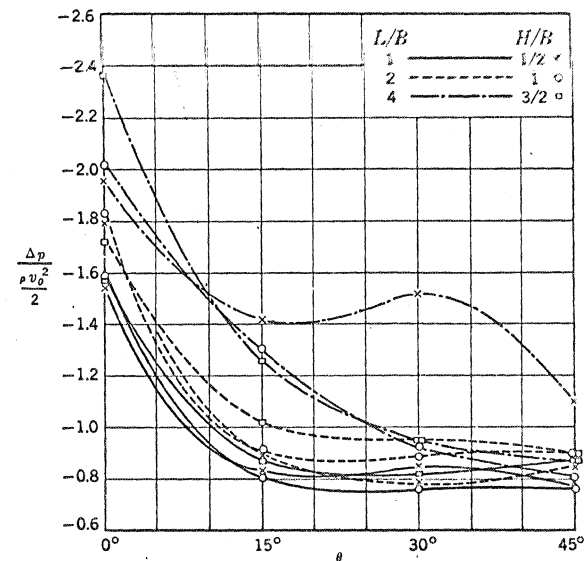


FIG. 8. Average negative pressure on transverse section of leeward roof is worst on flat-pitched roof and not greatly affected by building proportions.



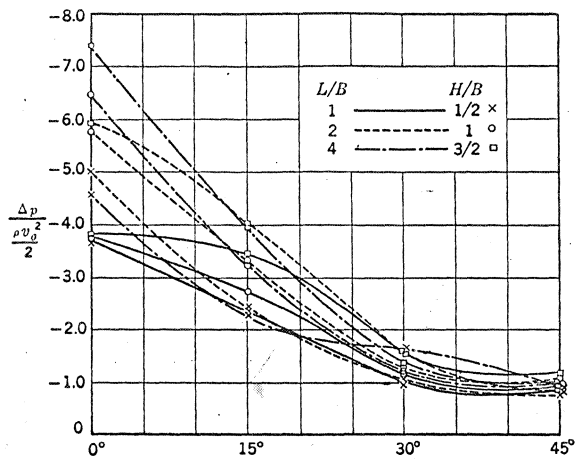


FIG. 9. Local pressure intensity on block building reaches extreme value in quartering wind. Roof pitch is significant below 30 deg.

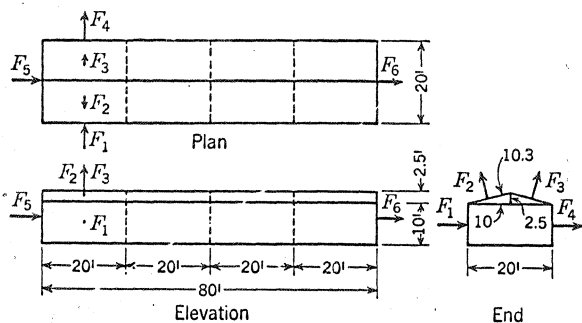


FIG. 10. Experimental coefficients are applied to 10 × 20 × 80-ft block building to determine wind forces.

in Fig. 2. A wind velocity of 100 mph (147 fps) is assumed.

Side thrust on a bent near the center of the building will be maximum when the wind angle  $\alpha = 0$ , or on an end bent when  $\alpha = 45$  deg. The average pressure coefficient for the front wall is found from Fig. 6 to be 0.84. The force  $F_1$  on a 10 × 20 ft panel will thus be

$$F_1 = 10 \times 20 \times 0.84 \times 0.0024 \times 147^2/2 = 4,350 \text{ lb per panel}$$

Maximum negative forces on the roof surfaces can be estimated from Figs. 7 and 8 for the 45-deg wind condition. Mean coefficients of -1.7 and -1.4 are read. These indicate the following forces:

$$F_2 = 10.3 \times 20 \times (-1.7) \times 0.0024 \times 147^2/2 = -9,100 \text{ lb per panel}$$

$$F_3 = 10.3 \times 20 \times (-1.4) \times 0.0024 \times 147^2/2 = -7,500 \text{ lb per panel}$$

Similarly, the force on the leeward wall at an end bent is

$$F_4 = 10 \times 20 \times (-0.9) \times 0.0024 \times 147^2/2 = -4,700 \text{ lb per panel}$$

These forces would be somewhat different at different bents but probably the same framing would be used

in order to make the construction uniform. The forces at any panel can be estimated by selecting coefficients from Fig. 2 and computing the total force in the manner illustrated above.

Longitudinal forces resulting from pressure on the ends of the building are based on an average pressure coefficient of 0.9 on one end and -0.2 on the other. The end areas are  $(10 \times 20) + (10 \times 2.5) = 225$  sq ft.

$$F_5 = 225 \times 0.9 \times 0.0024 \times 147^2/2 = 5,000 \text{ lb}$$

$$F_6 = 225 \times 0.2 \times 0.0024 \times 147^2/2 = 1,100 \text{ lb}$$

The large wind forces on the roof are opposite in direction to the dead load and are therefore not likely to be critical. It should be noted that such formulas as the commonly used Duchemin formula indicate the presence of downward forces which are added to the dead load, thereby causing roof supports to be considerably overdesigned.

Fastenings for wall and roof cover should be designed to resist the outward force caused by negative pressure outside the building accompanied by positive pressure inside due to the likelihood of an opening

on the windward face of the building. Inspection of Fig. 2 reveals the possibility of large vacuums near the ends and at the ridge of the roof, where the pressure coefficients range from -2.0 to -2.5. Elsewhere values vary from -1.0 to -1.5. If unity is added to these values to include the effect of stagnation pressure inside the building, it is apparent that a 100-mph wind may produce on the roof of this structure upward thrusts of from  $2.0 \times 0.0024 \times 147^2/2 = 52$  psf, to  $3.5 \times 0.0024 \times 147^2/2 = 90$  psf.

Outward forces are also exerted on the vertical walls, and average values are shown in Fig. 6, where a coefficient of 0.75 is indicated on the long side. This value may be used on all walls although nearly double this value may occur on particular areas, as shown in Fig. 2. If stagnation pressure inside is added, then it is seen that in a 100-mph wind the wall covering will be subjected to approximately

$$1.75 \times 0.0024 \times 147^2/2 = 45 \text{ psf.}$$

The systematic series of pressure diagrams that have been described provide a means of selecting safe and economical design wind loads on simple building forms of three common types. The detailed effect of geometrical configuration on pressure intensities is illustrated, particularly the presence of large vacuums in zones of separation. Furthermore, the tests on proximity imply a decided influence of adjacent buildings and indicate the necessity of special model studies on complex building forms or arrangements. Since the test results were measured in a steady wind, they do not indicate the extreme values that would result from gusts.

All experimental studies on which the accompanying diagrams are based were conducted in the laboratories of the Iowa Institute of Hydraulic Research. The majority of the tests on block structures were made by N. Chien, Y. Feng, and H. J. Wang as a master's thesis under the direction of the writer. The remaining tests were made by Messrs. Wang and T. T. Siao as an Institute project under the direction of Prof. Hunter Rouse and sponsored by the Office of Naval Research. Copies of the complete report by Chien, Feng, Wang, and Siao, under the title, "Wind-Tunnel Studies of Pressure Distribution on Elementary Building Forms," are available from the Iowa Institute of Hydraulic Research at the cost of reproduction, \$1.75 each.